Application of the black hole-fluid analogy: identification of a vortex flow through its characteristic waves

Theo Torres,[1] Sam Patrick,[1] Maurício Richartz,[2] and Silke Weinfurtner[1,3,4]

[1] *School of Mathematical Sciences, University of Nottingham, University Park, Nottingham, NG7 2RD, UK*
[2] *Centro de Matemática, Computação e Cognição, Universidade Federal do ABC (UFABC), 09210-170 Santo André, São Paulo, Brazil*
[3] *School of Physics and Astronomy, University of Nottingham, Nottingham, NG7 2RD, UK.*
[4] *Centre for the Mathematics and Theoretical Physics of Quantum Non-Equilibrium Systems, University of Nottingham, Nottingham, NG7 2RD, UK.*

Black holes are like bells; once perturbed they will relax through the emission of characteristic waves. The frequency spectrum of these waves is independent of the initial perturbation and, hence, can be thought of as a 'fingerprint' of the black hole. Since the 1970s scientists have considered the possibility of using these characteristic modes of oscillation to identify astrophysical black holes. Inspired by the black hole-fluid analogy, we demonstrate the universality of the black-hole relaxation process through the observation of characteristic modes emitted by a hydrodynamical vortex flow. The characteristic frequency spectrum is measured and agrees with theoretical predictions obtained using techniques developed for astrophysical black holes. Our findings allow for the first identification of a hydrodynamical vortex flow through its characteristic waves. The flow velocities inferred from the observed spectrum agree with a direct flow measurement. Our approach establishes a non-invasive method, applicable to vortex flows in fluids and superfluids alike, to identify the wave-current interactions and hence the effective field theories describing such systems.

***I*ntroduction and motivation.** According to General Relativity, the late stage of the relaxation process of an astrophysical black hole is expected to depend only on its mass and angular momentum, and not on the details of its formation process [1–3]. This opens up the possibility of *Black Hole Spectroscopy*: the identification of the spacetime geometry through the measurement of the frequency spectrum of gravitational waves emitted by a newly formed black hole [4–6]. With the recent detection of gravitational waves, this idea has started to turn into reality [7, 8]. Motivated by the black hole-fluid analogy, which implies that universal processes (e.g. Hawking radiation [9–11] and superradiance [12]) manifest themselves similarly in black holes and condensed matter systems, we apply the black hole spectroscopy idea to a vortex fluid flow.

The analogy, built on the works of Unruh [13] and Visser [14], relies on the fact that perturbations of some condensed matter systems, e.g. shallow water waves propagating on the free surface of an irrotational vortex flow [15], are mathematically equivalent to scalar waves propagating around a rotating black hole (see [16] for a review). Such a vortex flow, commonly called a draining bathtub (DBT) flow, is uniquely described by the velocity field $\mathbf{v}(t,r,\theta)=\mathbf{v}(r)=-\frac{\mathrm{D}}{r}\hat{\boldsymbol{r}}+\frac{\mathrm{C}}{r}\hat{\boldsymbol{\theta}}$. The two parameters, denoted C (for circulation) and D (for drain), are analogous to the angular momentum and mass of a rotating black hole. In fact, the region where the flow is sufficiently fast to trap any wave trying to escape from it is analogous to the event horizon of a black hole. Similarly, the region where the flow is sufficiently fast that waves are dragged along the flow direction is analogous to the ergosphere of a rotating black hole.

Once perturbed, a vortex flow will relax through the emission of surface waves that propagate on the air-water interface. Such waves correspond to small deformations, $\delta h(t,\mathbf{x})$, of the unperturbed surface elevation, where t denotes time and $\mathbf{x}$ represents the spatial coordinates on the two-dimensional free surface. For axisymmetric free surface vortex, it is convenient to adopt polar coordinates $\mathbf{x}=(r,\theta)$ and decompose the perturbations in terms of its azimuthal components,

$$\delta h(t,r,\theta)=\mathrm{Re}\left[\sum_{m\in\mathbb{Z}}\delta h_m(t,r)e^{im\theta}\right], \tag{1}$$

where the azimuthal number $m\in\mathbb{Z}$ indicates an m-fold symmetry with respect to the polar angle θ.

Towards the end of the relaxation process, each azimuthal component is well-approximated (in an open system) by a superposition of time-decaying modes, called *quasinormal modes* (QNMs) [1–3]. Each QNM oscillates at the characteristic frequency f_{mn} and has an amplitude that decays exponentially in time with a characteristic timescale of $1/\Gamma_{mn}$. The overtone number $n\in\mathbb{N}$ classifies the QNMs according to their decay times. The set of complex frequencies $\omega_{\mathrm{QNM}}(m,n)=2\pi f_{mn}+i\Gamma_{mn}$ is called the QNM spectrum. For the DBT flow, the QNMs have been extensively studied and their spectrum was calculated using various methods [17, 18]. The QNM spectra of more realistic vortex flows, either due to the presence of vorticity [19] or dispersion [20], have also been investigated.

One of the techniques available to estimate the QNM spectrum of a black hole is based on the properties of *light-rings* (LRs) [21, 22]. The LRs of a black hole are the orbits (i.e. the equilibrium points in the radial direc-

tion) of massless particles. The relation between QNMs and LR modes comes from the fact that, in many (but not all [23]) spacetimes, QNMs can be seen as waves travelling on the unstable orbits and slowly leaking out [2]. For a fluid flow, these modes can also be identified as the lowest energy modes capable of propagating across the entire flow (see Supplemental Material [24]). As such, they constitute the most favourable channel to transfer energy in and out of the system. While QNMs strongly rely on the openness of the system, the LR modes, being independent of the boundary conditions, do not. In particular, the presence of a non-open boundary condition, either at infinity or at the horizon, will modify the late-time behaviour of the relaxation process. More precisely, the decay times of characteristic waves will be altered by reflections from the boundaries.

Additionally, their non-oscillatory behaviour will be further modified by damping in the system and recurring perturbations. The oscillatory part of the LR spectrum, $f_\star(m)$, therefore provides a more robust quantity to characterise the fluid flow in finite size experiments. By proving the existence of LR modes in fluid flows[1], and by using their oscillation frequencies to extract flow parameters, our experiment provides a practical realisation of the black hole spectroscopy idea. Even though we expect the analogue of an event horizon to be present inside the vortex core, our analysis does not require the knowledge of its precise location. Indeed, our calculations are based on the general relativistic concept of light-rings, which is independent of the notion of an event horizon and does not depend on its properties.

Experimental setup. We set up a vortex flow out of equilibrium to observe the emission of characteristic modes during its relaxation. We call such a restless fluid flow an *Unruh vortex*[2]. Our experiment was conducted in a 3 m long and 1.5 m wide rectangular tank with a 2 cm-radius sink hole at the centre. Water is pumped continuously from one corner at a flow rate of 15 ± 1 ℓ/min. The sink-hole is covered until the water raises to a height of 10.00 ± 0.05 cm. Water is then allowed to drain, leading to the formation of an Unruh vortex. We recorded the perturbations of the free surface when the flow was in a quasi-stationary state at a water depth of 5.55 ± 0.05 cm. The water elevation was recorded using the Fast-Chequerboard Demodulation method [25] and the entire procedure was repeated 25 times.

The resulting Unruh vortex is axisymmetric to a good approximation, allowing us to perform an azimuthal decomposition, as in (1), to study its characteristic modes. We select specific azimuthal modes by performing a polar Fourier transform and we extract the associated radial profiles $\delta h_m(t, r)$. Azimuthal modes with $m > 0$ are co-rotating with the flow while modes with $m < 0$ are counter-rotating with the flow. By calculating the time Fourier transform of $\delta h_m(t, r)$, we estimate the *Power Spectral Density* (PSD) of each m-mode for $r \in [7.4 \text{ cm}, 25 \text{ cm}]$. In Fig. 1 we present the PSDs of a single experiment for a range of co- and counter-rotating modes (see Supplemental Material [24] for data analysis and flow characterisation).

Results. We can identify two different behaviours depending on the sign of m. For negative m's, the PSDs are approximately constant over the window of observation. The spectral density is peaked around a single frequency, which allows us to define the position-independent spectrum $f_{\text{peak}}(m)$ shown in Fig. 2. This spectrum can be used twofold. First, by employing a standard *Particle Imaging Velocimetry* (PIV) technique, we estimate the circulation parameter to be $C \approx 151$ cm^2/s and the drain parameter to be negligible, i.e. $D \approx 0$ cm^2/s (see Supplemental Material [24]). Using these values we can predict the characteristic mode spectrum $f_\star^{PIV}(m)$ using the LR properties, as shown by the dashed orange curve in Fig. 2. We observe that the model describing the characteristic oscillations of an Unruh vortex as LR modes is consistent with the data. This is the first experimental observation of the oscillatory part of the LR spectrum.

Second, after having validated our approach, we perform analogue black hole spectroscopy to characterise the fluid flow (as an alternative to PIV). By leaving the flow parameters C and D unspecified, we look for the best match (in terms of non-linear regression analysis) between the experimental spectrum $f_{\text{peak}}(m)$ of counter-rotating modes and the corresponding theoretical predictions for the LR spectrum. This reduces the DBT parameter space from two dimensions to one, constraining the flow parameters C and D to lie on the red curve shown in Fig. 3. Any pair of points along this curve will give the same spectrum, $f_\star^{BM}(m)$, represented by the solid black curve in Fig. 2. The region between the dashed orange curves shown in Fig. 3 represents the 95% confidence intervals for the values of C and D. This region overlaps the yellow rectangle which represents the possible flow parameters found using PIV. Note that, in this case, the black hole spectroscopy method imposes a slightly stronger constraint on the circulation parameter than PIV.

We highlight that in order to uniquely determine C and D the positive m part of the LR spectrum is also needed [26]. However, when the flow is characterised by only one parameter (e.g. purely rotating superfluids), the counter-rotating LR modes contain all the information about the fluid velocity. We note that this is effectively the case in our experiment. Since $D \ll C$ in our window of observation, the vortex flow can be considered to be

[1] Even though these are surface water waves and not electromagnetic waves, we shall still refer to them as LR modes due to the fluid-gravity analogy.

[2] This name comes from the German word "Unruhe" which means restlessness and was chosen in acknowledgment of W. G. Unruh, the founder of analogue gravity.

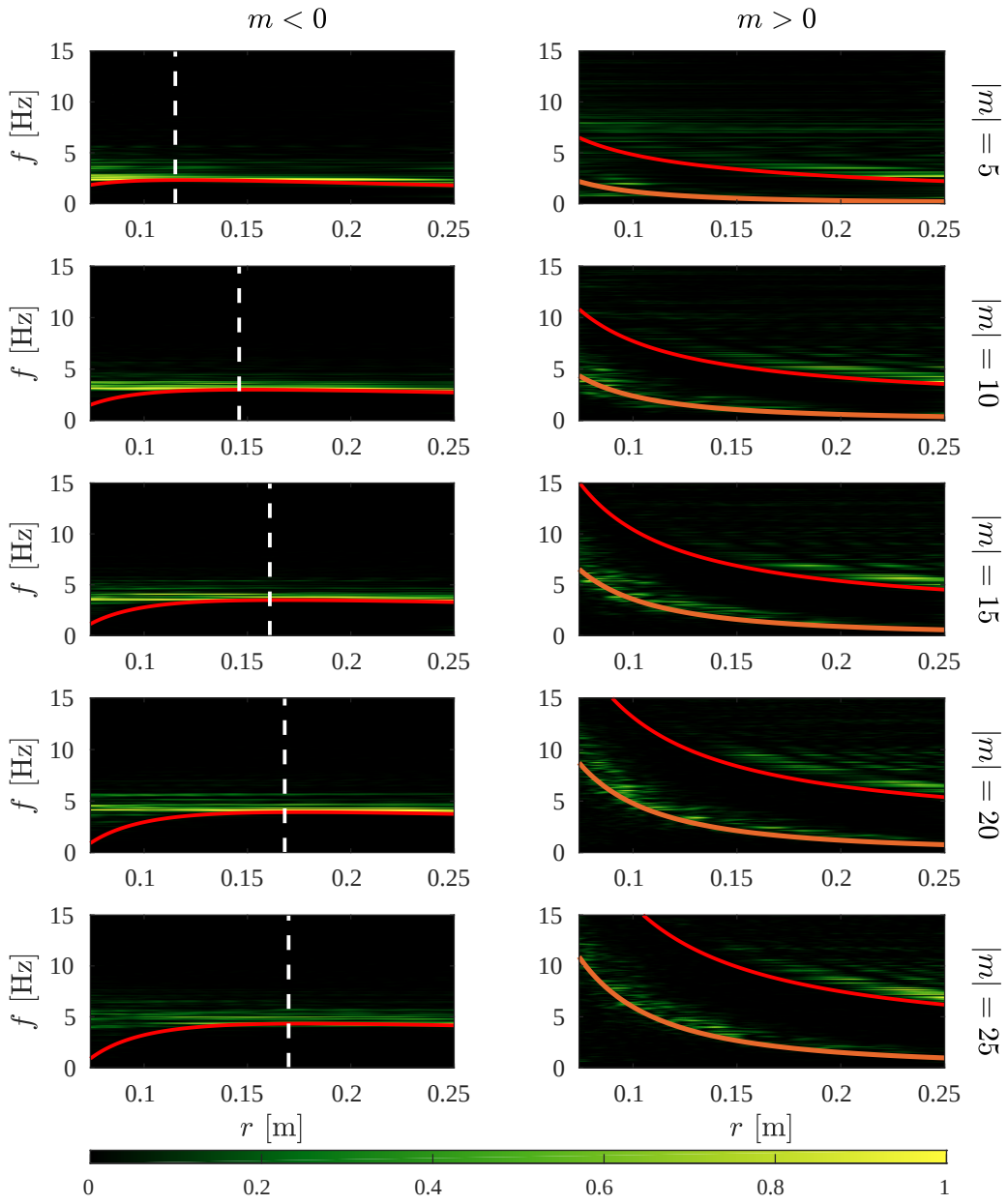

FIG. 1. **Normalised power spectral densities**. The power spectral density is compared with the minimum energy curve $f^+_{\rm min}(m,r)$, plotted in red, for various m. The maxima of $f^+_{\rm min}(m,r)$ indicate the location of the light-rings, $r_{LR}(m)$, which are shown in dashed white lines. For $m<0$, the spectral density peaks and the minimum energy line are distinguishable for small radii. For $m>0$, we observe two signals whose peaks are radius-dependent. The upper one follows the minimum energy line and corresponds, most probably, to random noise generated locally. The lower one follows the angular velocity of the fluid flow according to $f_\alpha(m,r) = mv^\theta(r)/(2\pi r)$ (orange curve) and is likely sourced by potential vorticity perturbations.

purely rotating and our observations are sufficient to fully characterise the flow in this region.

Although the LR modes are absent in the PSDs of the co-rotating modes shown in Fig. 1, two distinct, radius-dependent, signals are present. We can understand their origin using the flow parameters previously obtained. By computing the minimum energy line, $f^+_{\rm min}(m,r)$ (red curve), we observe that one of the signals corresponds to random noise generated locally. The other signal is related to the angular velocity of the fluid flow and can be matched with the curve $f_\alpha(m,r) = mv^\theta(r)/(2\pi r)$, shown in orange. This peak lies below the minimum energy and, hence, corresponds to evanescent modes. A possible explanation for their appearence is that *potential vorticity*

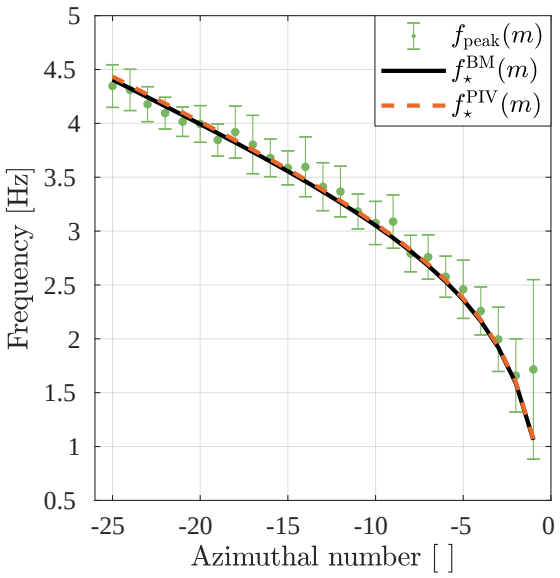

FIG. 2. **Characteristic spectrum of the Unruh vortex**. The frequency spectrum $f_{\rm peak}(m)$, extracted from the experimental data and represented by green dots, is compared with the theoretical prediction for the light-ring frequencies, $f_\star(m)$. The error bars indicate the standard deviation over 25 experiments. The dashed orange curve is the predicted spectrum, $f_\star^{\rm PIV}(m)$, computed for C = 151 cm^2/s and D = 0 cm^2/s. These flow parameters were obtained via an independent flow measurement, in our case Particle Imaging Velocimetry (PIV). The two spectra agree, confirming the detection of light-ring mode oscillations. The solid black curve, $f_\star^{\rm BM}(m)$, is the non-linear regression of the experimental data to the draining bathtub vortex model, and provides the values for C and D presented in the red curve of Fig. 3.

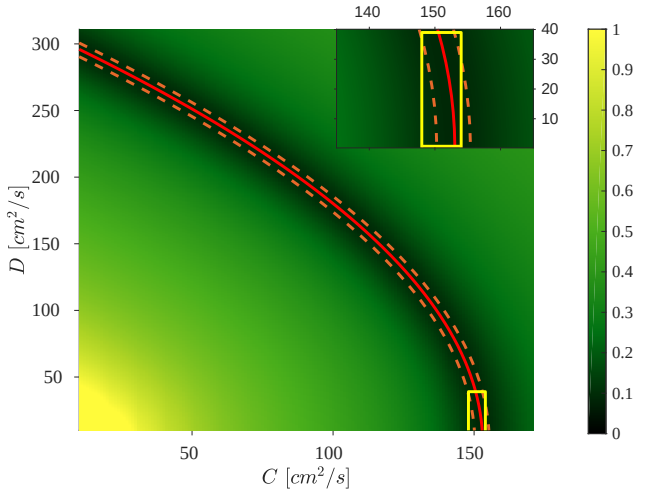

FIG. 3. **Flow characterisation**. The intensity of the background image represents the normalised weighted sum of squared residuals between the experimental spectrum, $f_{\rm peak}(m)$, and the theoretical prediction for the light-ring frequencies, $f_\star(m)$, as a function of the flow parameters. The red curve represents the family of possible values for C and D that best match the experimental data (using the method of weighted least squares). The area delimited by the dashed orange curves represents the 95% bootstrap confidence interval (see Supplemental Material [24]). It overlaps with the yellow rectangle on the bottom right corner, which corresponds to the flow parameters obtained using Particle Imaging Velocimetry. The spread along the C-direction represents the 95% confidence interval estimated via the likelihood function. The spread along the D-direction represents the extracted upper bound for D. In the top right corner we present a detailed view of the parameter space where the two flow measurements overlap.

(PV) perturbations act as a source for them [27]. In irrotational flows (which is the regime in which our observations are made), PV is carried by the flow as a passive tracer. Various m components of PV will therefore source free-surface deformations which are transported at frequencies $f_\alpha(m, r)$. These observations strengthen our confidence in the flow parameters obtained.

Final remarks. Our experiment exhibits a new facet of the fluid-gravity analogy [13–15] which has led to a better understanding of fundamental phenomena such as Hawking radiation [28, 29] and superradiance [30, 31]. Besides providing the first observation of light-ring mode oscillations, this successful demonstration of the principle behind black hole spectroscopy paves the way for real-life applications of the fluid-gravity analogy. This method can be used as an alternative to the standard fluid flow visualisation techniques, such as particle imaging velocimetry, that require tracer particles. In particular, when suitable tracer particles are hardly found or do not exist, like in superfluids [32], this is a promising non-invasive method to characterise fluid flows.

Acknowledgements. We are indebted to the technical and administrative staff in the School of Physics & Astronomy where our experimental setup is hosted. In particular, we want to thank Terry Wright, Tommy Napier and Ian Taylor for their support, hard work and sharing their technical knowledge and expertise with us to set up the experiment in Nottingham. Furthermore we would like to thank Antonin Coutant, Sam Dolan, Sebastian Erne, Zack Fifer, Harry Goodhew, Cisco Gooding, Jörg Schmiedmayer, Ralf Schützhold, Thomas Sotiriou, and Bill Unruh for the many discussions on all aspects of the project. For comments on the paper, we wish to thank Michael Berry, Sebastian Erne, Juan Garrahan, Kostas Kokkotas, Luis Lehner, Igor Lesanovsky and Bill Unruh.

M. R. acknowledges financial support from the São Paulo Research Foundation (FAPESP, Brazil), Grants No. 2013/09357-9 and 2018/10597-8, and from Conselho Nacional de Desenvolvimento Cientìfico e Tecnológico (CNPq, Brazil), Grant FA 309749/2017-4. M. R. is also

grateful to the University of Nottingham for hospitality while this work was being completed. SW acknowledges financial support provided under the Paper Enhancement Grant at the University of Nottingham, the Royal Society University Research Fellow (UF120112), the Nottingham Advanced Research Fellow (A2RHS2), the Royal Society Project (RG130377) grants, the Royal Society Enhancement Grant (RGF/EA/180286) and the EPSRC Project Grant (EP/P00637X/1). SW acknowledges partial support from STFC consolidated grant No. ST/P000703/.

[1] K. D. Kokkotas and B. G. Schmidt, Quasinormal modes of stars and black holes, Living Rev. Rel. **2**, 2 (1999), arXiv:gr-qc/9909058 [gr-qc].

[2] E. Berti, V. Cardoso, and A. O. Starinets, Quasinormal modes of black holes and black branes, Class. Quant. Grav. **26**, 163001 (2009), arXiv:0905.2975 [gr-qc].

[3] R. A. Konoplya and A. Zhidenko, Quasinormal modes of black holes: From astrophysics to string theory, Rev. Mod. Phys. **83**, 793 (2011), arXiv:1102.4014 [gr-qc].

[4] W. H. Press and K. S. Thorne, Gravitational-wave astronomy, Ann. Rev. Astron. Astrophys. **10**, 335 (1972).

[5] F. Echeverria, Gravitational-wave measurements of the mass and angular momentum of a black hole, Phys. Rev. D **40**, 3194 (1989).

[6] B. S. Sathyaprakash and B. F. Schutz, Physics, astrophysics and cosmology with gravitational waves, Living Reviews in Relativity **12**, 2 (2009).

[7] B. P. Abbott *et al.* (Virgo, LIGO Scientific), Observation of Gravitational Waves from a Binary Black Hole Merger, Phys. Rev. Lett. **116**, 061102 (2016), arXiv:1602.03837 [gr-qc].

[8] B. P. Abbott *et al.* (Virgo, LIGO Scientific), Properties of the Binary Black Hole Merger GW150914, Phys. Rev. Lett. **116**, 241102 (2016), arXiv:1602.03840 [gr-qc].

[9] S. Weinfurtner, E. W. Tedford, M. C. J. Penrice, W. G. Unruh, and G. A. Lawrence, Measurement of stimulated Hawking emission in an analogue system, Phys. Rev. Lett. **106**, 021302 (2011), arXiv:1008.1911 [gr-qc].

[10] J. Steinhauer, Observation of quantum Hawking radiation and its entanglement in an analogue black hole, Nature Phys. **12**, 959 (2016), arXiv:1510.00621 [gr-qc].

[11] L.-P. Euvé, F. Michel, R. Parentani, T. G. Philbin, and G. Rousseaux, Observation of noise correlated by the hawking effect in a water tank, Phys. Rev. Lett. **117**, 121301 (2016).

[12] T. Torres, S. Patrick, A. Coutant, M. Richartz, E. W. Tedford, and S. Weinfurtner, Observation of superradiance in a vortex flow, Nature Phys. **13**, 833 (2017), arXiv:1612.06180 [gr-qc].

[13] W. Unruh, Experimental black hole evaporation, Phys. Rev. Lett. **46**, 1351 (1981).

[14] M. Visser, Acoustic propagation in fluids: An Unexpected example of Lorentzian geometry, ArXiv: gr-qc/9311028 (1993), arXiv:gr-qc/9311028 [gr-qc].

[15] R. Schützhold and W. G. Unruh, Gravity wave analogues of black holes, Phys. Rev. D **66**, 044019 (2002).

[16] C. Barceló, S. Liberati, and M. Visser, Analogue gravity, Living Reviews in Relativity **14**, 3 (2011).

[17] E. Berti, V. Cardoso, and J. P. S. Lemos, Quasinormal modes and classical wave propagation in analogue black holes, Phys. Rev. **D70**, 124006 (2004), arXiv:gr-qc/0408099 [gr-qc].

[18] S. R. Dolan, L. A. Oliveira, and L. C. B. Crispino, Resonances of a rotating black hole analogue, Phys. Rev. **D 85**, 044031 (2012), arXiv:1105.1795 [gr-qc].

[19] S. Patrick, A. Coutant, M. Richartz, and S. Weinfurtner, Black hole quasibound states from a draining bathtub vortex flow, Phys. Rev. Lett. **121**, 061101 (2018), arXiv:1801.08473 [gr-qc].

[20] T. Torres, A. Coutant, S. Dolan, and S. Weinfurtner, Waves on a vortex: rays, rings and resonances, J. Fluid Mech. **857**, 291 (2018), arXiv:1712.04675 [gr-qc].

[21] C. J. Goebel, Comments on the "vibrations" of a Black Hole., Astrophys. J. **172**, L95 (1972).

[22] V. Cardoso, A. S. Miranda, E. Berti, H. Witek, and V. T. Zanchin, Geodesic stability, lyapunov exponents, and quasinormal modes, Phys. Rev. D **79**, 064016 (2009).

[23] G. Khanna and R. H. Price, Black Hole Ringing, Quasinormal Modes, and Light Rings, Phys. Rev. **D95**, 081501 (2017), arXiv:1609.00083 [gr-qc].

[24] See Supplemental Material at [url], which includes Refs. [19, 20, 22, 25, 33–39], for more details on the data analysis performed in this work, on the theory behind the experiment - including the properties of light-rings, and on the implementation of Particle Imaging Velocimetry in our experiment.

[25] S. Wildeman, Real-time quantitative Schlieren imaging by fast Fourier demodulation of a checkered backdrop, Experiments in Fluids **59**, 97 (2018), arXiv:1712.05679 [physics.flu-dyn].

[26] T. Torres, S. Patrick, M. Richartz, and S. Weinfurtner, Analogue black hole spectroscopy; or, how to listen to dumb holes, Classical and Quantum Gravity **36**, 194002 (2019).

[27] S. Churilov and Y. Stepanyants, Scattering of surface shallow water waves on a draining bathtub vortex, ArXiv: 1810.09796 (2018), arXiv:1810.09796 [physics.flu-dyn].

[28] T. Jacobson, Black hole evaporation and ultrashort distances, Phys. Rev. **D44**, 1731 (1991).

[29] W. G. Unruh, Sonic analog of black holes and the effects of high frequencies on black hole evaporation, Phys. Rev. **D51**, 2827 (1995).

[30] S. Basak and P. Majumdar, 'Superresonance' from a rotating acoustic black hole, Class. Quant. Grav. **20**, 3907 (2003).

[31] S. Basak and P. Majumdar, Reflection coefficient for superresonant scattering, Class. Quant. Grav. **20**, 2929 (2003).

[32] K. L. Chopra and J. B. Brown, Suspension of particles in liquid helium, Phys. Rev. **108**, 157 (1957).

[33] S. R. Dolan and E. S. Oliveira, Scattering by a draining bathtub vortex, Phys. Rev. **D87**, 124038 (2013).

[34] M. Richartz, A. Prain, S. Liberati, and S. Weinfurtner, Rotating black holes in a draining bathtub: superradiant scattering of gravity waves, Phys. Rev. **D91**, 124018 (2015), arXiv:1411.1662 [gr-qc].

[35] B. Efron and R. Tibshirani, Bootstrap methods for standard errors, confidence intervals, and other measures of statistical accuracy, Statistical Science **1**, 54 (1986).

[36] M. Raffel, C. Willert, F. Scarano, C. Kähler, S. Wereley, and J. Kompenhans, *Particle Image Velocimetry: A Practical Guide*, Experimental Fluid Mechanics

(Springer International Publishing, 2018).
[37] A. Andersen, T. Bohr, B. Stenum, J. J. Rasmussen, and B. Lautrup, Anatomy of a bathtub vortex, Phys. Rev. Lett. **91**, 104502 (2003).
[38] A. Andersen, T. Bohr, B. Stenum, J. J. Rasmussen, and B. Lautrup, The bathtub vortex in a rotating container, Journal of Fluid Mechanics **556**, 121 (2006).
[39] L. Cristofano, M. Nobili, G. Romano, and G. Caruso, Investigation on bathtub vortex flow field by particle image velocimetry, Experimental Thermal and Fluid Science **74**, 130 (2016).